Published in final edited form as:

Sci Signal. 2023 November 14; 16(811): eadh9399. doi:10.1126/scisignal.adh9399.

Vasodilators activate the anion channel TMEM16A in endothelial cells to reduce blood pressure

Alejandro Mata-Daboin[1], **Tessa A. C. Garrud**[1], **Carlos Fernandez-Pena**[1], **Dieniffer Peixoto-Neves**[1], **M. Dennis Leo**[1], **Angelica K. Bernardelli**[1], **Purnima Singh**[2], **Kafait U. Malik**[2], **Jonathan H. Jaggar**[1,*]

[1]Department of Physiology, University of Tennessee Health Science Center, Memphis TN 38163

[2]Department of Pharmacology, University of Tennessee Health Science Center, Memphis TN 38163

Abstract

Systemic blood pressure is acutely controlled by total peripheral resistance as determined by the diameter of small arteries and arterioles, the contractility of which is regulated by endothelial cells lining the lumen of blood vessels. We investigated the physiological functions of the chloride (Cl^-) channel TMEM16A in endothelial cells. TMEM16A channels generated calcium (Ca^{2+})-activated Cl^- currents in endothelial cells from control (*TMEM16A*$^{fl/fl}$) mice that were absent in those from mice with tamoxifen-inducible, endothelial cell-specific knockout of TMEM16A (*TMEM16A* ecKO). TMEM16A currents in endothelial cells were activated by the muscarinic receptor agonist acetylcholine and an agonist of the Ca^{2+} channel TRPV4, which localized in nanoscale proximity with TMEM16A as assessed by single molecule localization imaging of endothelial cells. Acetylcholine stimulated TMEM16A currents by activating Ca^{2+} influx through surface TRPV4 channels without altering the nanoscale properties of TMEM16A and TRPV4 surface clusters or their colocalization. In pressurized arteries, activation of TMEM16A channels in endothelial cells induced by acetylcholine, TRPV4 channel stimulation, or intraluminal ATP, another vasodilator, produced hyperpolarization and dilation. Furthermore, deficiency of TMEM16A channels in endothelial cells resulted in increased systemic blood pressure in conscious mice. These data indicate that vasodilators stimulate TRPV4 channels, leading to Ca^{2+}-dependent activation of nearby TMEM16A channels in endothelial cells to produce arterial hyperpolarization, vasodilation, and reduced blood pressure. Thus, TMEM16A is an anion channel in endothelial cells that regulates arterial contractility and blood pressure.

INTRODUCTION

Endothelial cells line the lumen of all blood vessels and regulate several physiological functions, including contractility, which controls regional organ blood flow and systemic

*Corresponding author: jjaggar@uthsc.edu.

Author Contributions: Conceptualization: JHJ, AM-D. Methodology: AM-D, TACG, CF-P, DP-N, MDL, AKB, PS. Investigation: AM-D, TACG, CF-P, DP-N, MDL, AKB, PS. Funding acquisition: JHJ, KUM, AM-D, TACG. Project administration: JHJ. Supervision: JHJ, KUM Writing – original draft: JHJ, AM-D, TACG. Writing – review & editing: JHJ, KUM, AM-D, TACG, CF-P, DP-N, MDL, AKB, PS.

Competing Interests: The authors declare that they have no competing interests.

pressure. Various receptor ligands, extracellular substances and mechanical stimuli act on endothelial cells to regulate their functions (1). Endothelial cells electrically couple to smooth muscle cells in the vascular wall and can directly modulate arterial potential to regulate contractility (2). Endothelial cells also produce and release several diffusible vasoactive factors, including nitric oxide (NO), a dilator (3). Given that endothelial cells regulate arterial contractility and blood pressure, it is essential to identify mechanisms by which vasoactive stimuli modulate their excitability.

Endothelial cells express several cation channels that regulate membrane potential and plasma membrane calcium (Ca^{2+}) influx to control arterial contractility. Cation channels present in endothelial cells include TRP vanilloid 4 (TRPV4), TRP polycystin 1 (TRPP1; also known as PKD2 and polycystin 2), TRP ankyrin 1 (TRPA1), and small (SK) and intermediate (IK) conductance Ca^{2+}-activated potassium channels (4–6). In contrast, the molecular identity and physiological functions of anion channels in endothelial cells are poorly understood. Chloride (Cl^-) is the predominant extracellular and intracellular anion. Cl^- currents were first identified in cultured vascular endothelial cells more than two decades ago (7–9). Ca^{2+}-activated Cl^- currents, volume-regulated Cl^- currents, and ClC currents have been detected in cultured endothelial cells (7, 8, 10, 11). Currently, it is unclear whether non-cultured endothelial cells generate Cl^- currents, the molecular identities of the channels that may produce these Cl^- currents and their physiological functions.

TMEM16A (also known as anoctamin 1) is a Ca^{2+}-activated homodimeric Cl^- channel expressed by the *TMEM16A* gene (12–17). TMEM16A channels have been proposed to generate Cl^- currents in cultured endothelial cells from tissues including human umbilical vein, heart and brain (18–20). Global deletion of *TMEM16A* in mice leads to several phenotypes, including repressed gastrointestinal tract peristalsis and tracheal abnormalities (21–23). Constitutive knockout of TMEM16A channels in endothelial cells does not alter the contractility of wire-mounted aortic rings or modify the blood pressure of mice as measured using a tail-cuff plethysmograph (18). However, the constitutive knockout of ion channels can lead to compensatory mechanisms that obscure and complicate attempts to identify their vascular functions (24–27). Similarly, the physiological function of TMEM16A channels in the resistance vasculature may differ from that in the aorta, which is a conduit vessel. Thus, alternative approaches to study TMEM16A channels in endothelial cells may reveal that these Cl^- channels regulate arterial contractility and blood pressure.

Here, we generated mice with a tamoxifen-inducible, endothelial cell-specific TMEM16A knockout to investigate the physiological functions of this ion channel in the resistance vasculature. Our data demonstrated that vasodilators activated TRPV4 channels, leading to Ca^{2+} influx which stimulated TMEM16A channels in endothelial cells. TMEM16A channels generated Cl^- currents which induced membrane hyperpolarization, vasodilation, and a reduction in blood pressure. We also showed that TMEM16A and TRPV4 clusters exhibited nanoscale overlap in the endothelial cell plasma membrane, providing evidence for local Ca^{2+}-dependent coupling between these ion channels. These results identify TMEM16A as an anion channel expressed in endothelial cells that regulates arterial contractility and blood pressure.

RESULTS

Generation and validation of tamoxifen-inducible, endothelial cell-specific TMEM16A knockout mice

Mice were genetically modified to insert loxP sites between exons 5 and 6 of the *TMEM16A* gene (*TMEM16A*$^{fl/fl}$). *TMEM16A*$^{fl/fl}$ mice were crossed with *Cdh5-Cre/ERT2* mice, a tamoxifen-inducible, endothelial cell-specific Cre line, generating *TMEM16A*$^{fl/fl}$:ecCre^{+} mice. Genomic PCR indicated that tamoxifen activated *TMEM16A* recombination in *TMEM16A*$^{fl/fl}$:ecCre^{+} (*TMEM16A* ecKO) mice but not in *TMEM16A*$^{fl/fl}$ mice (Fig. S1A). Western blotting experiments determined that TMEM16A protein in mesenteric arteries of tamoxifen-treated *TMEM16A* ecKO mice was ~75.8% of that in arteries of tamoxifen-treated *TMEM16A*$^{fl/fl}$ mice (Fig. 1A and 1B). This reduction is expected because TMEM16A is present in other cell types, including arterial smooth muscle cells, where recombination would not occur (28). Arteries of mice with tamoxifen-inducible smooth muscle cell-specific *TMEM16A* knockout have ~25% of the TMEM16A protein found in those of *TMEM16A*$^{fl/fl}$ control mice (29). Together, these observations suggest that ~25 % of total TMEM16A protein is present in endothelial cells of resistance-size systemic arteries. In contrast, the protein abundance of TRPV4, endothelial nitric oxide synthase (eNOS), IK, and SK3 was unaltered in the arteries of tamoxifen-treated *TMEM16A*$^{fl/fl}$:ecCre^{+} mice when compared to that in *TMEM16A*$^{fl/fl}$ mice (Fig. 1A and 1B). TMEM16A immunolabeling was detected in endothelial cells of en face mesenteric arteries from tamoxifen-treated *TMEM16A*$^{fl/fl}$ mice but was negligible in endothelial cells of arteries from *TMEM16A* ecKO mice (Fig. 1C).

TMEM16A channels produce Ca^{2+}-activated Cl^{-} currents in endothelial cells

Patch-clamp electrophysiology was performed to measure whole-cell Cl^{-} currents (I_{Cl}) in fresh-isolated mesenteric artery endothelial cells of *TMEM16A*$^{fl/fl}$ and *TMEM16A* ecKO mice. With 100 nM free Ca^{2+} present in the pipette solution, I_{Cl} was small in endothelial cells of *TMEM16A*$^{fl/fl}$ mice (Fig. S1B and S1C). Increasing the free Ca^{2+} concentration in the pipette solution from 100 nM to 1 μM elevated I_{Cl} density from 4.1 ± 0.9 to 28.0 ± 2.8 pA/pF, or ~6.83-fold in *TMEM16A*$^{fl/fl}$ endothelial cells at +80 mV (Fig. S1B and S1C). Tannic acid, a TMEM16A channel blocker, reduced this Ca^{2+}-activated I_{Cl} to ~30.4 % of control in *TMEM16A*$^{fl/fl}$ endothelial cells at +80 mV. In contrast, with 1 μM free Ca^{2+} in the pipette solution, I_{Cl} was small and insensitive to tannic acid in endothelial cells of *TMEM16A* ecKO mice (Fig. 1D, 1E and 1F). These results indicate that intracellular Ca^{2+} activates TMEM16A channels in endothelial cells of *TMEM16A*$^{fl/fl}$ mice but not in endothelial cells of *TMEM16A* ecKO mice.

ACh activates TRPV4-dependent TMEM16A currents in endothelial cells

Next, we studied the regulation of TMEM16A currents by vasodilators. Whole-cell I_{Cl} was measured using a pipette solution containing 100 nM free [Ca^{2+}] and a bath solution containing 2 mM Ca^{2+}. Acetylcholine (ACh), an endothelial cell-dependent vasodilator, increased I_{Cl} ~4.82-fold in endothelial cells of *TMEM16A*$^{fl/fl}$ mice. In contrast, ACh did not alter I_{Cl} in *TMEM16A* ecKO endothelial cells (Fig. 2A, 2B and 2C). Tannic acid or benzbromarone, another TMEM16A channel blocker, inhibited the I_{Cl} activated by ACh in

TMEM16A$^{fl/fl}$ endothelial cells (Fig. 2A, 2C, S2A and S2B). These data indicate that ACh stimulates TMEM16A-dependent I_{Cl} currents in endothelial cells.

ACh activates TRPV4 channels, leading to Ca^{2+} influx in endothelial cells (6, 30). We tested the hypothesis that ACh stimulates TRPV4 channels, which then activate TMEM16A currents. The TRPV4 channel blocker HC067047 inhibited ACh-induced I_{Cl} activation in endothelial cells of *TMEM16A*$^{fl/fl}$ mice (Fig. 2D and 2E). GSK1016790A (GSK101), a selective TRPV4 channel activator, stimulated a ~4.70-fold increase in I_{Cl} in *TMEM16A*$^{fl/fl}$ endothelial cells. In contrast to the effects in *TMEM16A*$^{fl/fl}$ cells, GSK101 activated a smaller ~1.90-fold increase in current that was not altered by tannic acid in *TMEM16A* ecKO endothelial cells (Fig. 2F, 2G and 2H). I_{Cl} activation by GSK101 was similarly inhibited by either tannic acid or the removal of extracellular Ca^{2+} in *TMEM16A*$^{fl/fl}$ endothelial cells (Fig. 2F, 2H and S2C). Because cesium (Cs^+) is the major cation present in the pipette solution, the small GSK101-induced current in *TMEM16A* ecKO endothelial cells may be due to Cs^+ current through TRPV4 channels (31). These results indicate that ACh stimulates TRPV4 channels, leading to Ca^{2+} influx which stimulates TMEM16A channels in endothelial cells.

TMEM16A and TRPV4 channel surface clusters are located in close spatial proximity in endothelial cells

Single-molecule localization microscopy (SMLM) in combination with total internal reflection fluorescence (TIRF) imaging was performed to measure the nanoscale properties and spatial proximity of surface TMEM16A and TRPV4 channel clusters in freshly isolated mesenteric artery endothelial cells. Imaging was performed on cells which labelled for CD31, an endothelial cell-specific marker, in oxygen scavenging photo-switching buffer (Fig. S3A). Localization precision of the Alexa Fluor-conjugated secondary antibodies used to label TMEM16A and TRPV4 channels were calculated to be between 15.9 and 19.1 nm in endothelial cells (Fig. S3B and S3C). The size of TMEM16A and TRPV4 surface clusters were similar at ~ 2646 and 2281 nm^2, respectively, in *TMEM16A*$^{fl/fl}$ endothelial cells (Fig. 3A and 3B). TMEM16A clusters were more numerous than TRPV4 clusters at 20.6 and 13.4 clusters/μm^2, respectively (Fig. 3C). The mean distance (center to center) between each TMEM16A cluster and its nearest TRPV4 neighbor was ~107 nm, indicating close spatial proximity (Fig. 3D). Approximately 17.8% of TMEM16A clusters overlapped with a TRPV4 cluster (Fig. 3E). When experimental data were reconstructed using Coste's randomization algorithm, TMEM16A and TRPV4 cluster overlap was only ~5.8 % (Fig. 3E). The size and density of TRPV4 clusters were similar in *TMEM16A*$^{fl/fl}$ and *TMEM16A* ecKO endothelial cells, indicating that TMEM16A knockout did not alter TRPV4 channel cluster properties (Fig. 3B and 3C). ACh did not alter the size or density of TMEM16A or TRPV4 clusters or the proximity or overlap of these clusters, indicating that Ca^{2+}-dependent signaling between TRPV4 and TMEM16A channels is not associated with changes in the spatial properties of clusters.

In *TMEM16A* ecKO endothelial cells, the mean size of TMEM16A clusters was ~19.0 % of that in *TMEM16A*$^{fl/fl}$ endothelial cells (Fig. 3B). TMEM16A clusters were far less numerous in *TMEM16A* ecKO endothelial cells, at ~6.9 % of that in *TMEM16A*$^{fl/fl}$

endothelial cells (Fig. 3C). The distance between TMEM16A and TRPV4 clusters was also much greater at ~544.8 nm, with only ~0.5 % of TMEM16A clusters displaying overlap with a TRPV4 cluster in *TMEM16A* ecKO endothelial cells (Fig. 3D and E). These data indicate that clusters observed in *TMEM16A* ecKO cells are due to background labeling of TMEM16A antibodies, validating the data obtained in $TMEM16A^{fl/fl}$ endothelial cells (Fig. 3A) (32). Moreover, these results demonstrate that surface TMEM16A and TRPV4 clusters locate in nanoscale proximity with a sizable proportion exhibiting overlap in the endothelial cell plasma membrane.

Endothelial cell TMEM16A channel activation leads to arterial hyperpolarization and vasodilation

Arterial membrane potential is a major determinant of contractility (33). We tested the hypothesis that endothelial cell TMEM16A channels regulate the membrane potential of pressurized (80 mmHg) third-order mesenteric arteries. Under unstimulated conditions, the membrane potential of $TMEM16A^{fl/fl}$ and *TMEM16A* ecKO arteries were similar at −32.2 and −31.0 mV, respectively (Fig. 4A and 4B). ACh stimulated a mean membrane hyperpolarization of ~ 7.5 mV in $TMEM16A^{fl/fl}$ arteries (Fig. 4A and 4B). In contrast, ACh-induced hyperpolarization in *TMEM16A* ecKO arteries was ~ 2.7 mV, or ~36.4 % of that in $TMEM16A^{fl/fl}$ arteries (Fig. 4A and 4B). Thus, ACh stimulates arterial hyperpolarization, in part, through the activation of endothelial cell TMEM16A channels.

Myography was performed on pressurized (80 mmHg) myogenic mesenteric arteries to investigate the regulation of arterial contractility by endothelial cell TMEM16A channels. ACh or intraluminal ATP stimulated vasodilation in *TMEM16A* ecKO arteries that was ~31.7 and 36.1%, respectively, of that in $TMEM16A^{fl/fl}$ arteries (Fig. 4C and 4D). In contrast, vasodilation to intraluminal flow (15 dyn/cm^2) was similar in $TMEM16A^{fl/fl}$ and *TMEM16A* ecKO arteries (Fig. 4C and D). Vasoconstriction to intravascular pressure (myogenic tone) or treatment with 60 mM K^+ or phenylephrine, which act on smooth muscle cells, were similar in $TMEM16A^{fl/fl}$ and *TMEM16A* ecKO arteries (Fig. S4A-D). These data demonstrate that endothelial cell-specific TMEM16A knockout does not cause generalized endothelial cell or smooth muscle cell dysfunction. Consistent with ACh acting on TRPV4 channels to stimulate TMEM16A currents in endothelial cells, GSK101 produced ~51.6% less dilation in *TMEM16A* ecKO mesenteric arteries than in those of $TMEM16A^{fl/fl}$ mice (Fig. 4C and 4D). ACh produced dilation that was substantially inhibited by HC067047 in pressurized arteries of $TMEM16A^{fl/fl}$ mice and less so in arteries of *TMEM16A* ecKO mice (Fig. 4D). These results indicate that ACh, ATP and TRPV4 channel activation stimulate TMEM16A channels in endothelial cells, leading to membrane hyperpolarization and vasodilation.

Endothelial cell TMEM16A channels reduce systemic blood pressure

Blood pressure was measured using radiotelemetry in conscious, freely-moving $TMEM16A^{fl/fl}$ and *TMEM16A* ecKO mice. Prior to tamoxifen-treatment, blood pressure was similar in $TMEM16A^{fl/fl}$ and *TMEM16A* ecKO mice (Fig. S5A). Following tamoxifen administration, mean arterial pressure was higher in *TMEM16A* ecKO mice than in $TMEM16A^{fl/fl}$ mice primarily due to an elevation in diastolic pressure (Fig. 5A and S5B).

In contrast, locomotor activity and heart rate were similar in *TMEM16A*$^{fl/fl}$ and *TMEM16A* ecKO mice (Fig. 5B and C). The mean arterial blood pressure elevation in *TMEM16A* ecKO mice occurred during both active (dark) and inactive (light) periods (Fig. 5D). These results indicate that endothelial cell TMEM16A channels reduce blood pressure in mice.

DISCUSSION

Here, we generated a tamoxifen-inducible, endothelial cell-specific TMEM16A knockout mouse model to investigate the physiological functions of this Cl^- channel in this cell type. We showed that ACh and ATP activated TMEM16A channels in endothelial cells, leading to vasorelaxation. TMEM16A and TRPV4 protein clusters located in nanoscale proximity in the plasma membrane of endothelial cells, with a substantial number exhibiting overlap. ACh activated TRPV4 channels, leading to Ca^{2+} influx which stimulated TMEM16A channels. TMEM16A channel activation in endothelial cells produced membrane hyperpolarization and vasodilation. We also demonstrated that TMEM16A channel knockout in endothelial cells elevated blood pressure in mice.

Cl^- currents have been recorded in cultured endothelial cells, including those from the aorta and pulmonary arteries (34). Ca^{2+}-activated Cl^- currents, volume-regulated Cl^- currents, and ClC currents are detected in cultured endothelial cells (7, 8, 10, 11). Cultured neonatal mouse cardiac endothelial cells, cultured brain endothelial cells and cultured human umbilical vein endothelial cells generate Cl^- currents which are sensitive to manipulations that include TMEM16A inhibitors, TMEM16A-targeting RNAi, and a TMEM16A pore-blocking antibody (18–20). Whether non-cultured endothelial cells generate Cl^- currents, the molecular identity of the proteins that generate these currents, and their physiological functions were unclear. Here, using genetic knockout and pharmacological approaches we showed that TMEM16A channels generate Ca^{2+}-activated Cl^- currents in fresh-isolated endothelial cells. Increasing intracellular Ca^{2+} concentration activated recombinant TMEM16A channels and reduced their outward rectification (12–14). Our data showed that at 100 nM free Ca^{2+}, TMEM16A currents were small. An increase in free Ca^{2+} to 1 μM stimulated TMEM16A currents which exhibited substantial outward rectification. Splice variation in TMEM16A channels modulated both the Ca^{2+} sensitivity and extent of outward rectification (35). Thus, endothelial cells appear to express splice variants of TMEM16A channels that exhibit these biophysical properties. Future studies should identify the splice variants of TMEM16A channels that are expressed in endothelial cells.

Our data showed that TRPV4-mediated Ca^{2+} influx activated TMEM16A channels in endothelial cells. We did not determine the mechanism by which ATP activated TMEM16A channels in mesenteric artery endothelial cells to cause vasodilation, but purinergic receptors activate TRPV4 channels in pulmonary artery endothelial cells, providing a potential explanation for these data (36). Our results suggest that endothelial cell TMEM16A channels do not contribute to flow-mediated vasodilation. Mechanical stimulation with a fluid stream activates a Cl^- current in cultured human aortic endothelial cells, although the molecular identity of the channels involved was not determined (37). Flow stimulates a protein complex composed of polycystin 1 (PKD1) and PKD2 in endothelial cells, leading to eNOS, SK, and IK channel activation and vasodilation (4, 32). Flow also stimulates Piezo1,

a Ca^{2+}-permeant non-selective cation channel, in both arterial and capillary endothelial cells (38, 39). Our data therefore suggest that a PKD1/PKD2 complex and Piezo1 may not signal to TMEM16A in endothelial cells. Flow may also activate Cl^- currents through different signaling mechanisms in non-cultured mesenteric artery endothelial cells and cultured aortic endothelial cells, indicating that further investigation of the mechanisms involved is required.

The binding of ACh to $G\alpha_{q/11}$-coupled muscarinic receptors can stimulate both TRPV4 channels on the plasma membrane and IP_3 receptors (IP_3Rs) on the endoplasmic reticulum, leading to an increase in intracellular Ca^{2+} concentration (6). We showed that TRPV4 channel inhibition blocked ACh-induced TMEM16A currents, pharmacological activation of TRPV4 channels using GSK101 activated TMEM16A currents, and that removing extracellular Ca^{2+} inhibited TRPV4-mediated TMEM16A channel activation. These data indicate that Ca^{2+} influx through TRPV4 channels stimulates TMEM16A currents in endothelial cells. SMLM imaging demonstrated that ~18 % of TMEM16A clusters overlap with a TRPV4 cluster, with the average distance from a TMEM16A cluster to its nearest TRPV4 neighbor 107 nm. At physiological voltages, the EC_{50} for Ca^{2+} of TMEM16A channels is in the hundreds of nanomolar to low micromolar concentration range (13, 35). In contrast, global intracellular Ca^{2+} concentration ranges between 34 and 220 nM nanomolar in non-cultured ECs (40). Thus, TMEM16A channels are likely to be activated by local intracellular Ca^{2+} transients generated by nearby TRPV4 channels, which are termed sparklets (6). In support of this concept, the pipette solution in our patch-clamp experiments contained EGTA, a slow Ca^{2+} chelator that buffers global Ca^{2+} signals but does not abolish local Ca^{2+} transients produced by Ca^{2+} channels (41). TMEM16A channels may also be activated by Ca^{2+} signals generated by other Ca^{2+} channels, such as endoplasmic reticulum IP_3Rs. Ca^{2+} influx through TRPV4 channels has been reported to trigger Ca^{2+}-induced Ca^{2+} release from IP_3Rs (42). Endoplasmic reticulum Ca^{2+} release may activate TMEM16A channels that are both nearby TRPV4 channels and those that are more distant from TRPV4 channels. Such an investigation is more suitable for a future study, particularly as the relative contributions of these different Ca^{2+} signaling mechanisms may depend on several factors, including the agonist used, its concentration, and the cell voltage, which determines the driving force for plasma membrane Ca^{2+} influx. In contrast, TMEM16A channel knockout did not affect flow-mediated vasodilation, even though TRPV4 channels contribute to this response (43–45). These data suggest that distinct populations of TRPV4 channels may exist: those that are activated by receptor agonists and stimulate TMEM16A channels and those that are activated by flow and do not stimulate TMEM16A channels.

ACh produced membrane hyperpolarization in pressurized arteries of *TMEM16A*$^{fl/fl}$ mice that was attenuated in arteries of *TMEM16A* ecKO mice. In contrast, activation of TMEM16A channels in smooth muscle cells lead to membrane depolarization and vasoconstriction (28). For TMEM16A channel activation to elicit hyperpolarization, the equilibrium potential for Cl^- (E_{Cl}) must be negative relative to physiological voltage to create a driving force for Cl^- influx. Intracellular Cl^- concentration in endothelial cells of pressurized mesenteric arteries does not appear to have been previously measured but it can be estimated when considering arterial membrane potential. At an intravascular pressure of 80 mmHg and with 122 mM Cl^- in the bath solution, the membrane potential of

TMEM16A$^{fl/fl}$ pressurized mesenteric arteries was ~−32.2 mV. Thus, intracellular Cl^- must be less than 34.8 mM for TMEM16A currents to produce hyperpolarization in endothelial cells.

TRPV4 channel activation stimulated SK and IK channels and eNOS signaling in endothelial cells, leading to membrane hyperpolarization and vasodilation (6, 27, 30). We showed that TMEM16A channels were another functional Ca^{2+}-activated downstream target of TRPV4 channels in endothelial cells. Our data showed that endothelial cell-specific TMEM16A channel knockout reduced ACh-, GSK101- and ATP-induced vasodilation by up to two-thirds. These observations raise the question of how the loss of one of several downstream targets of TRPV4 channels can robustly reduce agonist-induced vasodilation. One explanation is that TRPV4-activated SK, IK, and TMEM16A channels may act both in series and in parallel to amplify functional responses. Membrane hyperpolarization caused by SK, IK and TMEM16A channel activation would increase the driving force for TRPV4-mediated Ca^{2+} influx and thus, further stimulate each channel type. In agreement with this concept, IK and SK channels act in a positive-feedback manner to amplify ACh-induced Ca^{2+} signaling in endothelial cells, with the loss of one K^+ channel type sufficient to inhibit ACh-induced Ca^{2+} signaling (46). Here, our results showed that genetic ablation of TMEM16A channels in endothelial cells robustly attenuated the magnitude of ACh-induced membrane hyperpolarization and vasodilation. This may occur through the inhibition of a positive-feedback mechanism which normally amplifies SK and IK channel activation and perhaps eNOS. Future studies should investigate these possibilities.

Our results, which were obtained with a tamoxifen-inducible endothelial cell-specific TMEM16A knockout mouse, contrasted with those acquired with a constitutive (non-inducible) TMEM16A knockout mouse model (18). ACh-induced relaxation in wire-mounted, pre-constricted aortic rings was not altered by constitutive TMEM16A channel knockout (18). The aorta is a conduit vessel that does not develop myogenic tone or regulate blood pressure and in which endothelial cell TMEM16A channels may not regulate contractility. Preconstriction of wire-mounted aortic rings may have also inhibited TMEM16A channels in endothelial cells, thereby preventing their subsequent regulation of contractility. In contrast, we studied pressurized resistance-size mesenteric arteries that develop myogenic tone and regulate systemic blood pressure. Similarly, blood pressure measured using tail-cuff plethysmography did not differ between control and constitutive TMEM16A knockout mice (18). Tail cuff plethysmography is generally considered to be a less sensitive method than radiotelemetry, which was the method we used here to measure blood pressure. The use of a tail cuff may explain the lack of a blood pressure phenotype in the constitutive TMEM16A channel knockout mice (47, 48). We showed that tamoxifen-inducible knockout of endothelial cell TMEM16A channels increased blood pressure in mice. The increase we observed in mean arterial blood pressure in endothelial cell-specific TMEM16A knockout mice can be explained by an elevation in total peripheral resistance due to attenuated receptor-mediated vasodilation. Future studies should investigate the potential involvement of endothelial TMEM16A channels in other organ systems that regulate blood pressure, including the kidney and heart. Signaling compensation may have also occurred in constitutive TMEM16A knockout mice that nullified a contractility and blood pressure phenotype. Similar examples include mice with constitutive knockout of

TRPC6, TRPM4 and TRPV4 channels, which produce paradoxical effects on vascular contractility and blood pressure associated with compensatory mechanisms (24–27). Our data suggest that remodeling did not occur in arteries of *TMEM16A* ecKO mice. Tamoxifen-treatment reduced TMEM16A channel protein abundance without altering that of TRPV4, IK or SK3 channels or eNOS in mesenteric arteries. One limitation of tamoxifen-inducible Cre-driven models is that knockout may not occur uniformly in cells. Here, arterial wall TMEM16A protein in *TMEM16A* ecKO arteries was ~75% of that in *TMEM16A*$^{fl/fl}$ arteries. Tamoxifen-inducible smooth muscle cell-specific knockout of TMEM16A channels (*TMEM16A* smKO) reduced TMEM16A protein in resistance-size arteries to ~25% of that in *TMEM16A*$^{fl/fl}$ mice (29). These data support the conclusion that TMEM16A protein was essentially absent in mesenteric artery endothelial cells of *TMEM16A* ecKO mice.

A selectivity screen of several commonly used TMEM16A channel inhibitors (CaCCinh-A01, MONNA, Ani9, niclosamide, and niflumic acid) (49) suggested that all but one inhibitor, Ani9, block the sarco/endoplasmic reticulum Ca^{2+} ATPase and IP_3Rs (49). Interference with Ca^{2+} signaling may explain why previously published data were interpreted to suggest that these compounds block TMEM16A channels. Here, we used tannic acid and benzbromarone, which are TMEM16A channel inhibitors that were not screened in the aforementioned study. We also compared the effects of these inhibitors on both *TMEM16A*$^{fl/fl}$ and *TMEM16A* ecKO endothelial cells, which provided an important control.

In summary, we showed that physiological and pharmacological vasodilators activated TMEM16A channels in endothelial cells. Surface TMEM16A clusters located in nanoscale proximity with TRPV4 clusters and exhibited overlap, and Ca^{2+} influx through TRPV4 channels stimulated TMEM16A channels to elicit Cl^- currents. We also demonstrated that TMEM16A channel activation in endothelial cells caused arterial hyperpolarization, vasodilation, and a reduction in blood pressure. Thus, TMEM16A is an anion channel present in endothelial cells that regulates arterial contractility and blood pressure.

MATERIALS AND METHODS

Animals

Procedures were performed in accordance with the Institutional Animal Care and Use Committee (IACUC) at the University of Tennessee Health Science Center (Protocol # 23-0444). Mice with loxP sites inserted between exons 5 and 6 of the *TMEM16A gene* (*TMEM16A*$^{fl/fl}$) were custom-made for us by Taconic-Cyagen. *TMEM16A*$^{fl/fl}$ mice were crossed with *Cdh5-Cre/ERT2* mice, a tamoxifen-inducible, endothelial cell-specific Cre line, generating *TMEM16A*$^{fl/fl}$:ecCre+ mice. *Cdh5-CreERT2* mice were kindly provided by Cancer Research UK (50). The genotypes of all mice were confirmed using PCR (Transnetyx) before use. Mice (male, 12 weeks of age) were injected with tamoxifen [50 mg/kg, intraperitoneal (i.p.)] once per day for 5 days and studied between 14 and 21 days after the last injection.

Tissue preparation and EC isolation

Mice were euthanized with isoflurane (1.5%) followed by decapitation. First to fifth order mesenteric arteries were harvested, cleaned of adventitial tissue and immersed in ice-cold physiological solution with the following concentrations (in mM): 134 NaCl, 6 KCl, 2 $CaCl_2$, 1 $MgCl_2$, 10 HEPES, 10 glucose (pH 7.4). Endothelial cells were isolated by enzymatic dissociation of mesenteric arteries by incubating in a Ca^{2+}-free solution containing (in mM): 80 Na glutamate, 55 NaCl, 5.6 KCl, 10 HEPES, 10 glucose, 2 $MgCl_2$, pH 7.4 with 2 mg/ml protease and 0.33 mg/ml hyaluronidase for 20 minutes at 37 °C. Elastase was included for the last 5 minutes of incubation at a concentration of 0.1 mg/ml. After multiple washes using ice-cold Ca^{2+}-free isolation solution, arteries were minced and gently triturated. Isolated endothelial cells were maintained in ice-cold isolation solution and used within 6 hours.

Genomic PCR

Genomic DNA was isolated from brain homogenate using a Purelink Genomic DNA kit (Thermo Fisher Scientific). Reaction conditions used were initial denaturation at 95°C for 2 minutes followed by 45 cycles at 95°C for 0.5 min, 55°C for 0.5 min, 72°C for 5 min, and extension at 72°C for 10 min. The primer sequences used to identify floxed and deleted alleles in tamoxifen-treated *TMEM16A*$^{fl/fl}$ or *TMEM16A* ecKO mice were 5’-CTCAGGCAATCTCAGTGAAGC-3’ (forward) and 5’-GAACTGTCCTGGAGACACAGG-3’ (reverse).

Western blotting

Whole mesenteric arteries were dissected and placed into ice-cold RIPA buffer (Sigma-Aldrich, R0278) containing protease inhibitor cocktail (Sigma-Aldritch, P8340). Arteries were cut with scissors and homogenized with an A0001 tissue homogenizer (Argos Technologies). The resulting lysate was centrifuged at 4 °C, 12,000 rpm for 10 minutes, and the supernatant was assayed for protein concentration. Samples were heated in Laemelli buffer (Biorad, 1610747) at 100°C for 5 minutes prior to gel loading. Samples were run on 7.5% SDS-polyacrylamide gels and proteins were transferred onto nitrocellulose membranes. Membranes were blocked with 5% milk for 1 hour and incubated overnight at 4°C with primary antibody for TMEM16A (Cell Signaling Technology, D1M9Q), TRPV4 (Sigma Aldrich, MABS466), eNOS (Abcam, ab76198), IK (Alomone, APC-064), SK3 (Sigma Aldrich, P0608) or actin (Cell Signaling Technology, E4D9Z). Membranes were washed and incubated with secondary antibodies at room temperature for 45 minutes. ECL substrate (Thermofisher, 34095) was added to membranes and bands were imaged using a ChemiDoc Touch Imaging System (Bio-Rad). Quantification of protein bands was done using ImageJ (NIH) software. Protein bands were normalized to the corresponding actin band.

En face arterial immunofluorescence

Arteries were cut longitudinally and fixed with 4% paraformaldehyde in PBS for 1 hour. After washing with PBS, the arteries were permeabilized with 0.2% TritonX-100, blocked with 5% goat serum and incubated overnight at 4°C with TMEM16A (Cell Signaling,

D1M9Q) and CD31 (Abcam, ab7388) primary monoclonal antibodies. Arteries were incubated with Alexa Fluor 488 donkey anti-rat secondary antibody (Thermo Fisher) and Alexa Fluor 555 donkey anti-rabbit secondary antibody (Thermo Fisher) for 1 hour at room temperature. Segments were washed with PBS, oriented on slides with the endothelial layer downwards and mounted in 80% glycerol solution. Alexa 488 and Alexa 555 were excited at 488 and 555 with emission collected at 488-540 nm and ≥555 nm, respectively, using a Zeiss LSM 710 laser-scanning confocal microscope.

Patch-clamp electrophysiology

Freshly isolated endothelial cells were allowed to adhere to a glass coverslip in a recording chamber. Macroscopic Cl^- currents were measured using the conventional whole-cell configuration applying voltage ramps (0.13 mV/ms) between −80 to +80 mV from a holding potential of −40 mV. The pipette solution contained (in mM): 10 CsCl, 130 Cs aspartate, 10 HEPES, 10 glucose, 1 EGTA, 1 MgATP, and 0.2 NaGTP (pH 7.2 adjusted with CsOH). Total Mg^{2+} was adjusted to give a final free concentration of 1 mM and total Ca^{2+} was adjusted to give a final free concentration of 100 nM or 1 μM, depending on the experimental condition. Free Mg^{2+} and Ca^{2+} were calculated using WebmaxC Standard. The bath solution contained 140 NMDG-Cl, 10 HEPES, 10 glucose, 1 $MgCl_2$, and 2 $CaCl_2$ (pH 7.4). Ca^{2+}-free bath solution was the same composition as the bath solution except Ca^{2+} was omitted and 1 mM EGTA added. Membrane currents were recorded using an Axopatch 200B amplifier, Digidata 1332A, and Clampex 10.3 (Molecular Devices). Currents were filtered at 5 kHz and normalized to membrane capacitance. Liquid junction potential was corrected offline. Experiments were performed at room temperature (22°C). Offline analysis was performed using Clampfit 10.4.

Single-molecule localization microscopy

Freshly isolated mesenteric artery endothelial cells were allowed to adhere to 35 mm glass-bottom dishes, fixed in 4% paraformaldehyde, and permeabilized with 0.5% Triton X-100 PBS solution. After blocking with 5 % BSA, the cells were immunolabelled overnight at 4°C using primary antibodies to TMEM16A (Cell Signaling, D1M9Q), CD31 (Abcam, ab7388) and TRPV4 (Sigma Aldrich, MABS466). Alexa Fluor 488 donkey anti-mouse, Alexa Fluor 555 goat anti-rat, and Alexa Fluor 647 donkey anti-rabbit antibodies were used for detection. ONI Bcubed buffers A+B (ONI) were mixed at the time of the experiment, added to the cells to acquire the images, and replaced every hour. A super-resolution Zeiss Elyra 7 microscope equipped with 488 nm (500 mW), 561 nm (500 mW), and 642 nm (500 mW) lasers was used to capture the images with a 63x Plan-Apochromat (NA 1.46) oil immersion lens and a CMOS camera. The camera was operated in frame-transfer mode at a rate of 100 Hz with an exposure time of 30 ms. TIRF mode was used with emission band-pass filters of 550–650 and 660–760 nm.

CD31 labeling (Alexa 488) was acquired with lattice-SIM to identify endothelial cells that were then used for SMLM imaging. Reconstruction of lattice-SIM images was performed using the SIM processing tool of ZEN software (Zeiss black edition).

Localization precision of fluorophores was calculated using $\sigma^2_{x,y}=[(s^2+q^2/12)/N]+[(8\pi s^4 b^2)/(q^2N^2)]$, where $\sigma_{x,y}$ is the localization precision of a fluorescent probe in lateral dimensions, s is the standard deviation of the point-spread function, N is the total number of photons gathered, q is the pixel size in the image space, and b is the background noise per pixel. The precision of localization is proportional to DLR/√N, where DLR is the diffraction-limited resolution of a fluorophore and N is the average number of detected photons per switching event, assuming the point-spread functions are Gaussian. 30,000 images were used to reconstruct TMEM16A and TRPV4 clusters. This was done by fitting signals to a Gaussian function and applying a point spread function calculated with a standardized 40 nm bead slide using ZEN Black software (Zeiss). The first 2500 frames were excluded to allow for the photo-switching probes to stabilize. Software drift correction was applied using model-based cross-correlation. Data were analyzed using ImageJ v2.1.0 (NIH) and the JACoP v2.0 plugin by selecting “Objects based methods”. Cluster proximity was calculated as the distance between the center of each TRPV4 cluster and its nearest TMEM16A neighbor.

Pressurized artery myography

Isolated third-order mesenteric arteries segments that were 1-2 mm in length were cannulated at each end in a perfusion chamber (Living Systems Instrumentation), continuously perfused at 37 °C with physiological saline solution (PSS) that contained (in mM): 112 NaCl, 6 KCl, 24 $NaHCO_3$, 1.8 $CaCl_2$, 1.2 $MgSO_4$, 1.2 KH_2PO_4 and 10 glucose, and gassed with 21% O_2, 5% CO_2 and 74% N_2 to maintain pH at 7.4. A Servo pump model PS-200-P (Living Systems) was used to modify intravascular pressure, which was monitored through pressure transducers. Arterial diameter was recorded at a frequency of 1 Hz using a Nikon TS100-F microscope equipped with a CCD camera and the automatic edge-detection function of IonWizard software (Ionoptix). Myogenic tone was calculated as: 100×(1−Dactive/Dpassive) where Dactive is active arterial diameter and Dpassive is the diameter determined in the presence of Ca^{2+}-free PSS supplemented with 5 mM EGTA.

Pressurized artery membrane potential measurements

Membrane potential was measured in pressurized (80 mmHg) myogenic third-order mesenteric arteries following the development of stable myogenic tone. A sharp glass microelectrode with a resistance between 50-90 MOhm was filled with 3M KCl and inserted into the adventitial side of the arterial wall. Successful intracellular impalements were determined by the following criteria: a sharp negative deflection in potential upon insertion, voltage stability for at least one minute after entry, a sharp positive voltage deflection upon exit from the recorded cell and a < 10% change in tip resistance after the impalement. Membrane potential was acquired using a WPI FD223a amplifier and digitized using a MiniDigi 1A USB interface controlled by pClamp 9.2 software (Axon Instruments).

Telemetric blood pressure and locomotion measurements

Radio transmitters (PA-C10, Data Sciences International) were implanted subcutaneously into anesthetized mice, with the sensing electrode placed in the aorta through the left carotid artery. Mice were allowed to recover for 7-10 days. Blood pressure was then recorded every 10 s for 7 days prior to tamoxifen injection and again for 14 days after the last tamoxifen

injection (50 mg/kg per day for 5 consecutive days, i.p) using a PhysioTel Digital telemetry platform (Data Sciences International). Dataquest A.R.T. software was used to acquire and analyze data.

Statistical analysis

Statistical analysis was performed using Graphpad Prism software. Data are expressed as means ± SE. Normality of data distribution was assessed with Kolmogorov-Smirnov test. Paired and unpaired data from two populations were compared using Student t-test, while ANOVA with Tukey post hoc test was used for multiple group comparisons. Differences were considered significant at $P<0.05$.

Supplementary Material

Refer to Web version on PubMed Central for supplementary material.

Acknowledgments:

We thank the Advanced Imaging Core at the University of Tennessee Health Science Center for technical assistance during super resolution imaging experiments.

Funding:

This work was funded by NIH/NHLBI grants HL155180, HL155186, and HL166411 to J.H.J. and HL019134-46 to K.U.M. and American Heart Association (AHA) Postdoctoral Fellowships AHA 830462 to A.M.-D. and AHA 1014035 to T.A.G.

Data and Materials Availability:

All data needed to evaluate the conclusions in the paper are present in the paper or the Supplementary Materials. *Cdh5(PAC)-CreERT2* mice were kindly provided by Ralf Adams of Cancer Research UK under an MTA.

References and Notes

1. Durand MJ, Gutterman DD, Diversity in mechanisms of endothelium-dependent vasodilation in health and disease. Microcirculation 20, 239–247 (2013); published online EpubApr (10.1111/micc.12040). [PubMed: 23311975]
2. Garland CJ, Hiley CR, Dora KA, EDHF: spreading the influence of the endothelium. British journal of pharmacology 164, 839–852 (2011); published online EpubOct (10.1111/j.1476-5381.2010.01148.x). [PubMed: 21133895]
3. Vane JR, The Croonian Lecture, 1993. The endothelium: maestro of the blood circulation. Philosophical transactions of the Royal Society of London. Series B, Biological sciences 343, 225–246 (1994); published online EpubJan 29 (10.1098/rstb.1994.0023). [PubMed: 8146236]
4. MacKay CE, Leo MD, Fernandez-Pena C, Hasan R, Yin W, Mata-Daboin A, Bulley S, Gammons J, Mancarella S, Jaggar JH, Intravascular flow stimulates PKD2 (polycystin-2) channels in endothelial cells to reduce blood pressure. eLife 9, (2020); published online EpubMay 4 (10.7554/eLife.56655).
5. Sullivan MN, Gonzales AL, Pires PW, Bruhl A, Leo MD, Li W, Oulidi A, Boop FA, Feng Y, Jaggar JH, Welsh DG, Earley S, Localized TRPA1 channel Ca^{2+} signals stimulated by reactive oxygen species promote cerebral artery dilation. Sci Signal 8, ra2 (2015); published online EpubJan 6 (10.1126/scisignal.2005659). [PubMed: 25564678]
6. Sonkusare SK, Bonev AD, Ledoux J, Liedtke W, Kotlikoff MI, Heppner TJ, Hill-Eubanks DC, Nelson MT, Elementary Ca^{2+} signals through endothelial TRPV4 channels regulate vascular

function. Science 336, 597–601 (2012); published online EpubMay 4 (10.1126/science.1216283). [PubMed: 22556255]

7. Nilius B, Szucs G, Heinke S, Voets T, Droogmans G, Multiple types of chloride channels in bovine pulmonary artery endothelial cells. J. Vasc. Res 34, 220–228 (1997); published online Epub5/1997 [PubMed: 9226304]
8. von Weikersthal SF, Barrand MA, Hladky SB, Functional and molecular characterization of a volume-sensitive chloride current in rat brain endothelial cells. The Journal of physiology 516 (Pt 1), 75–84 (1999); published online EpubApr 1 (10.1111/j.1469-7793.1999.075aa.x). [PubMed: 10066924]
9. Zhong N, Fang QZ, Zhang Y, Zhou ZN, Volume- and calcium-activated chloride channels in human umbilical vein endothelial cells. Acta Pharmacol Sin 21, 215–220 (2000); published online EpubMar [PubMed: 11324418]
10. Nilius B, Sehrer J, Droogmans G, Permeation properties and modulation of volume-activated Cl(−)-currents in human endothelial cells. British journal of pharmacology 112, 1049–1056 (1994); published online EpubAug (10.1111/j.1476-5381.1994.tb13189.x). [PubMed: 7952863]
11. Lamb FS, Clayton GH, Liu BX, Smith RL, Barna TJ, Schutte BC, Expression of CLCN voltage-gated chloride channel genes in human blood vessels. J Mol Cell Cardiol 31, 657–666 (1999); published online EpubMar (10.1006/jmcc.1998.0901). [PubMed: 10198195]
12. Caputo A, Caci E, Ferrera L, Pedemonte N, Barsanti C, Sondo E, Pfeffer U, Ravazzolo R, Zegarra-Moran O, Galietta LJ, TMEM16A, a membrane protein associated with calcium-dependent chloride channel activity. Science 322, 590–594 (2008); published online Epub10/24/2008 [PubMed: 18772398]
13. Yang YD, Cho H, Koo JY, Tak MH, Cho Y, Shim WS, Park SP, Lee J, Lee B, Kim BM, Raouf R, Shin YK, Oh U, TMEM16A confers receptor-activated calcium-dependent chloride conductance. Nature 455, 1210–1215 (2008); published online Epub10/30/2008 [PubMed: 18724360]
14. Schroeder BC, Cheng T, Jan YN, Jan LY, Expression cloning of TMEM16A as a calcium-activated chloride channel subunit. Cell 134, 1019–1029 (2008); published online Epub9/19/2008 [PubMed: 18805094]
15. Dang S, Feng S, Tien J, Peters CJ, Bulkley D, Lolicato M, Zhao J, Zuberbuhler K, Ye W, Qi L, Chen T, Craik CS, Jan YN, Minor DL Jr., Cheng Y, Jan LY, Cryo-EM structures of the TMEM16A calcium-activated chloride channel. Nature 552, 426–429 (2017); published online EpubDec 21 (10.1038/nature25024). [PubMed: 29236684]
16. Paulino C, Kalienkova V, Lam AKM, Neldner Y, Dutzler R, Activation mechanism of the calcium-activated chloride channel TMEM16A revealed by cryo-EM. Nature 552, 421–425 (2017); published online EpubDec 21 (10.1038/nature24652). [PubMed: 29236691]
17. Sheridan JT, Worthington EN, Yu K, Gabriel SE, Hartzell HC, Tarran R, Characterization of the oligomeric structure of the Ca(2+)-activated Cl− channel Ano1/TMEM16A. The Journal of biological chemistry 286, 1381–1388 (2011); published online EpubJan 14 (10.1074/jbc.M110.174847). [PubMed: 21056985]
18. Ma MM, Gao M, Guo KM, Wang M, Li XY, Zeng XL, Sun L, Lv XF, Du YH, Wang GL, Zhou JG, Guan YY, TMEM16A Contributes to Endothelial Dysfunction by Facilitating Nox2 NADPH Oxidase-Derived Reactive Oxygen Species Generation in Hypertension. Hypertension 69, 892–901 (2017); published online EpubMay (10.1161/HYPERTENSIONAHA.116.08874). [PubMed: 28320851]
19. Wu MM, Lou J, Song BL, Gong YF, Li YC, Yu CJ, Wang QS, Ma TX, Ma K, Hartzell HC, Duan DD, Zhao D, Zhang ZR, Hypoxia augments the calcium-activated chloride current carried by anoctamin-1 in cardiac vascular endothelial cells of neonatal mice. British journal of pharmacology 171, 3680–3692 (2014); published online EpubAug (10.1111/bph.12730). [PubMed: 24758567]
20. Suzuki T, Yasumoto M, Suzuki Y, Asai K, Imaizumi Y, Yamamura H, TMEM16A Ca^{2+}-Activated Cl- Channel Regulates the Proliferation and Migration of Brain Capillary Endothelial Cells. Molecular pharmacology 98, 61–71 (2020); published online EpubJul (10.1124/mol.119.118844). [PubMed: 32358165]

21. Rock JR, Futtner CR, Harfe BD, The transmembrane protein TMEM16A is required for normal development of the murine trachea. Dev Biol 321, 141–149 (2008); published online EpubSep 1 (10.1016/j.ydbio.2008.06.009). [PubMed: 18585372]
22. Hwang SJ, Blair PJ, Britton FC, O'Driscoll KE, Hennig G, Bayguinov YR, Rock JR, Harfe BD, Sanders KM, Ward SM, Expression of anoctamin 1/TMEM16A by interstitial cells of Cajal is fundamental for slow wave activity in gastrointestinal muscles. The Journal of physiology 587, 4887–4904 (2009); published online EpubOct 15 (10.1113/jphysiol.2009.176198). [PubMed: 19687122]
23. Huang F, Rock JR, Harfe BD, Cheng T, Huang X, Jan YN, Jan LY, Studies on expression and function of the TMEM16A calcium-activated chloride channel. Proceedings of the National Academy of Sciences of the United States of America 106, 21413–21418 (2009); published online EpubDec 15 (10.1073/pnas.0911935106). [PubMed: 19965375]
24. Mathar I, Vennekens R, Meissner M, Kees F, Van der Mieren G, Camacho Londono JE, Uhl S, Voets T, Hummel B, van den Bergh A, Herijgers P, Nilius B, Flockerzi V, Schweda F, Freichel M, Increased catecholamine secretion contributes to hypertension in TRPM4-deficient mice. J. Clin. Invest 120, 3267–3279 (2010); published online Epub9/1/2010 [PubMed: 20679729]
25. Dietrich A, Mederos YS, Gollasch M, Gross V, Storch U, Dubrovska G, Obst M, Yildirim E, Salanova B, Kalwa H, Essin K, Pinkenburg O, Luft FC, Gudermann T, Birnbaumer L, Increased vascular smooth muscle contractility in TRPC6$^{-/-}$ mice. Mol. Cell Biol 25, 6980–6989 (2005); published online Epub8/2005 [PubMed: 16055711]
26. Nishijima Y, Zheng X, Lund H, Suzuki M, Mattson DL, Zhang DX, Characterization of blood pressure and endothelial function in TRPV4-deficient mice with L-NAME and angiotensin II-induced hypertension. Physiol Rep 2, e00199 (2014); published online Epub1/1/2014 ([PubMed: 24744878]
27. Earley S, Pauyo T, Drapp R, Tavares MJ, Liedtke W, Brayden JE, TRPV4-dependent dilation of peripheral resistance arteries influences arterial pressure. Am. J. Physiol Heart Circ. Physiol 297, H1096–H1102 (2009); published online Epub9/2009 [PubMed: 19617407]
28. Bulley S, Jaggar JH, Cl− channels in smooth muscle cells. Pflugers Arch 466, 861–872 (2014); published online Epub5/2014 [PubMed: 24077695]
29. Leo MD, Peixoto-Nieves D, Yin W, Raghavan S, Muralidharan P, Mata-Daboin A, Jaggar JH, TMEM16A channel upregulation in arterial smooth muscle cells produces vasoconstriction during diabetes. American journal of physiology. Heart and circulatory physiology 320, H1089–H1101 (2021); published online EpubMar 1 (10.1152/ajpheart.00690.2020). [PubMed: 33449847]
30. Zhang DX, Mendoza SA, Bubolz AH, Mizuno A, Ge ZD, Li R, Warltier DC, Suzuki M, Gutterman DD, Transient receptor potential vanilloid type 4-deficient mice exhibit impaired endothelium-dependent relaxation induced by acetylcholine in vitro and in vivo. Hypertension 53, 532–538 (2009); published online EpubMar (10.1161/HYPERTENSIONAHA.108.127100). [PubMed: 19188524]
31. Voets T, Prenen J, Vriens J, Watanabe H, Janssens A, Wissenbach U, Bodding M, Droogmans G, Nilius B, Molecular determinants of permeation through the cation channel TRPV4. The Journal of biological chemistry 277, 33704–33710 (2002); published online EpubSep 13 (10.1074/jbc.M204828200). [PubMed: 12093812]
32. MacKay CE, Floen M, Leo MD, Hasan R, Garrud TAC, Fernandez-Pena C, Singh P, Malik KU, Jaggar JH, A plasma membrane-localized polycystin-1/polycystin-2 complex in endothelial cells elicits vasodilation. eLife 11, (2022); published online EpubMar 1 (10.7554/eLife.74765).
33. Nelson MT, Patlak JB, Worley JF, Standen NB, Calcium channels, potassium channels, and voltage dependence of arterial smooth muscle tone. Am. J. Physiol 259, C3–18 (1990); published online Epub7/1990 [PubMed: 2164782]
34. Nilius B, Droogmans G, Calcium-activated chloride channels in vascular endothelial cells. Current Topics in Membranes 15, 327–344 (2002).
35. Ferrera L, Caputo A, Ubby I, Bussani E, Zegarra-Moran O, Ravazzolo R, Pagani F, Galietta LJ, Regulation of TMEM16A chloride channel properties by alternative splicing. J. Biol. Chem 284, 33360–33368 (2009); published online Epub11/27/2009 [PubMed: 19819874]
36. Daneva Z, Ottolini M, Chen YL, Klimentova E, Kuppusamy M, Shah SA, Minshall RD, Seye CI, Laubach VE, Isakson BE, Sonkusare SK, Endothelial pannexin 1-TRPV4 channel signaling lowers

pulmonary arterial pressure in mice. eLife 10, (2021); published online EpubSep 7 (10.7554/eLife.67777).

37. Nakao M, Ono K, Fujisawa S, Iijima T, Mechanical stress-induced Ca2+ entry and Cl− current in cultured human aortic endothelial cells. The American journal of physiology 276, C238–249 (1999); published online EpubJan (10.1152/ajpcell.1999.276.1.C238). [PubMed: 9886940]
38. Wang S, Chennupati R, Kaur H, Iring A, Wettschureck N, Offermanns S, Endothelial cation channel PIEZO1 controls blood pressure by mediating flow-induced ATP release. The Journal of clinical investigation 126, 4527–4536 (2016); published online EpubDec 1 (10.1172/JCI87343). [PubMed: 27797339]
39. Harraz OF, Klug NR, Senatore AJ, Hill-Eubanks DC, Nelson MT, Piezo1 Is a Mechanosensor Channel in Central Nervous System Capillaries. Circulation research 130, 1531–1546 (2022); published online EpubMay 13 (10.1161/CIRCRESAHA.122.320827). [PubMed: 35382561]
40. Socha MJ, Hakim CH, Jackson WF, Segal SS, Temperature effects on morphological integrity and Ca(2)(+) signaling in freshly isolated murine feed artery endothelial cell tubes. American journal of physiology. Heart and circulatory physiology 301, H773–783 (2011); published online EpubSep (10.1152/ajpheart.00214.2011). [PubMed: 21705671]
41. Stern MD, Buffering of calcium in the vicinity of a channel pore. Cell Calcium 13, 183–192 (1992); published online Epub3/1992 [PubMed: 1315621]
42. Heathcote HR, Lee MD, Zhang X, Saunter CD, Wilson C, McCarron JG, Endothelial TRPV4 channels modulate vascular tone by Ca^{2+} -induced Ca^{2+} release at inositol 1,4,5-trisphosphate receptors. British journal of pharmacology 176, 3297–3317 (2019); published online EpubSep (10.1111/bph.14762). [PubMed: 31177523]
43. Mendoza SA, Fang J, Gutterman DD, Wilcox DA, Bubolz AH, Li R, Suzuki M, Zhang DX, TRPV4-mediated endothelial Ca^{2+} influx and vasodilation in response to shear stress. American journal of physiology. Heart and circulatory physiology 298, H466–476 (2010); published online EpubFeb (10.1152/ajpheart.00854.2009). [PubMed: 19966050]
44. Kohler R, Heyken WT, Heinau P, Schubert R, Si H, Kacik M, Busch C, Grgic I, Maier T, Hoyer J, Evidence for a functional role of endothelial transient receptor potential V4 in shear stress-induced vasodilatation. Arteriosclerosis, thrombosis, and vascular biology 26, 1495–1502 (2006); published online EpubJul (10.1161/01.ATV.0000225698.36212.6a). [PubMed: 16675722]
45. Hartmannsgruber V, Heyken WT, Kacik M, Kaistha A, Grgic I, Harteneck C, Liedtke W, Hoyer J, Kohler R, Arterial response to shear stress critically depends on endothelial TRPV4 expression. PloS one 2, e827 (2007); published online EpubSep 5 (10.1371/journal.pone.0000827). [PubMed: 17786199]
46. Qian X, Francis M, Kohler R, Solodushko V, Lin M, Taylor MS, Positive feedback regulation of agonist-stimulated endothelial Ca2+ dynamics by KCa3.1 channels in mouse mesenteric arteries. Arteriosclerosis, thrombosis, and vascular biology 34, 127–135 (2014); published online EpubJan (10.1161/ATVBAHA.113.302506). [PubMed: 24177326]
47. Drueke TB, Devuyst O, Blood pressure measurement in mice: tail-cuff or telemetry? Kidney Int 96, 36 (2019); published online EpubJul (10.1016/j.kint.2019.01.018). [PubMed: 31229048]
48. Whitesall SE, Hoff JB, Vollmer AP, D'Alecy LG, Comparison of simultaneous measurement of mouse systolic arterial blood pressure by radiotelemetry and tail-cuff methods. American journal of physiology. Heart and circulatory physiology 286, H2408–2415 (2004); published online EpubJun (10.1152/ajpheart.01089.2003). [PubMed: 14962829]
49. Genovese M, Buccirossi M, Guidone D, De Cegli R, Sarnataro S, di Bernardo D, Galietta LJV, Analysis of inhibitors of the anoctamin-1 chloride channel (transmembrane member 16A, TMEM16A) reveals indirect mechanisms involving alterations in calcium signalling. British journal of pharmacology, (2022); published online EpubNov 29 (10.1111/bph.15995).
50. Wang Y, Nakayama M, Pitulescu ME, Schmidt TS, Bochenek ML, Sakakibara A, Adams S, Davy A, Deutsch U, Luthi U, Barberis A, Benjamin LE, Makinen T, Nobes CD, Adams RH, Ephrin-B2 controls VEGF-induced angiogenesis and lymphangiogenesis. Nature 465, 483–486 (2010); published online Epub5/27/2010 [PubMed: 20445537]

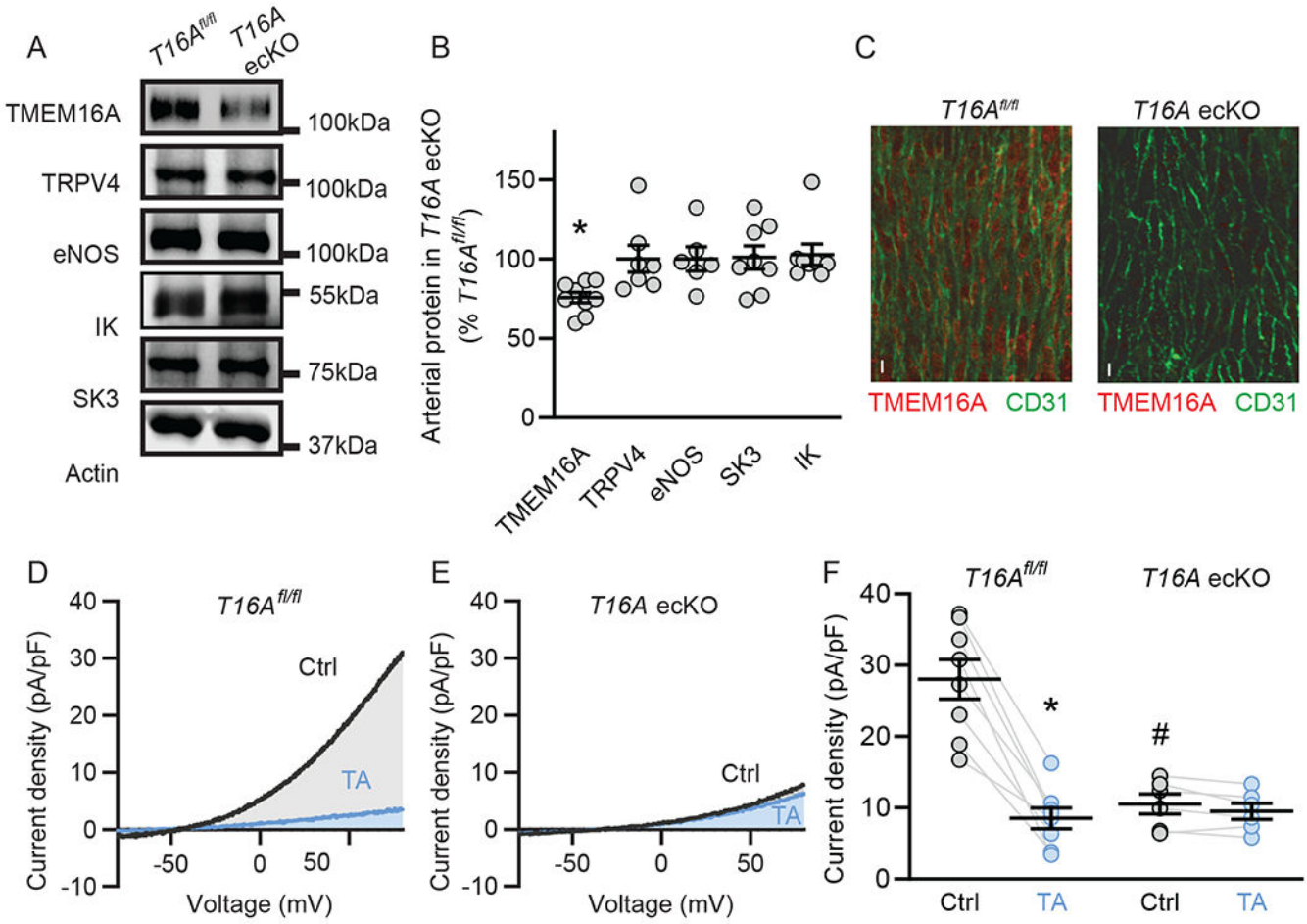

Fig. 1. Generation and validation of *TMEM16A* ecKO mice.

(**A**) Representative Western blots illustrating TMEM16A, TRPV4, eNOS, IK and SK3 proteins in mesenteric arteries of tamoxifen-treated *TMEM16A*$^{fl/fl}$ (*T16A*$^{fl/fl}$) and *TMEM16A* ecKO (*T16A* ecKO) mice. (**B**) Mean data for TMEM16A (n=9 mesenteric arteries from 9 *TMEM16A*$^{fl/fl}$ and 9 *TMEM16A* ecKO mice), TRPV4 (n=7 mesenteric arteries from 7 *TMEM16A*$^{fl/fl}$ and 7 *TMEM16A* ecKO mice), eNOS (n=6 mesenteric arteries from 6 *TMEM16A*$^{fl/fl}$ and 6 *TMEM16A* ecKO mice), SK3 (n=8 mesenteric arteries from 8 *TMEM16A*$^{fl/fl}$ and 8 *TMEM16A* ecKO mice), and IK (n=8 mesenteric arteries from 8 *TMEM16A*$^{fl/fl}$ and 8 *TMEM16A* ecKO mice) proteins in mesenteric arteries of tamoxifen-treated *TMEM16A* ecKO mice and tamoxifen-treated *TMEM16A*$^{fl/fl}$ mice. *, P<0.05 compared to *TMEM16A*$^{fl/fl}$. (**C**) En face immunofluorescence images of endothelial cells from mesenteric arteries in tamoxifen-treated *TMEM16A*$^{fl/fl}$ and *TMEM16A* ecKO mice (representative of 4 mesenteric arteries from 3 mice for each genotype). Labelling of CD31, an endothelial cell-specific specific marker, is also shown. Scale bars = 50 μm. (**D** and **E**) Representative whole-cell current recordings of freshly isolated endothelial cells from *TMEM16A*$^{fl/fl}$ (D) and *TMEM16A* ecKO (E) mice with 1 μM free Ca^{2+} in the pipette solution, before (black, Ctrl) and after (blue) applying tannic acid (TA, 10 μM) to the bath solution. (**F**) Mean data obtained from experiments in (D) and (E) at +80 mV. N=8 cells

from 7 *TMEM16A*$^{fl/fl}$ mice; n=6 cells from 6 *TMEM16A* ecKO mice. *, P<0.05 compared to Ctrl within genotype; #, P<0.05 compared to Ctrl in *TMEM16A*$^{fl/fl}$.

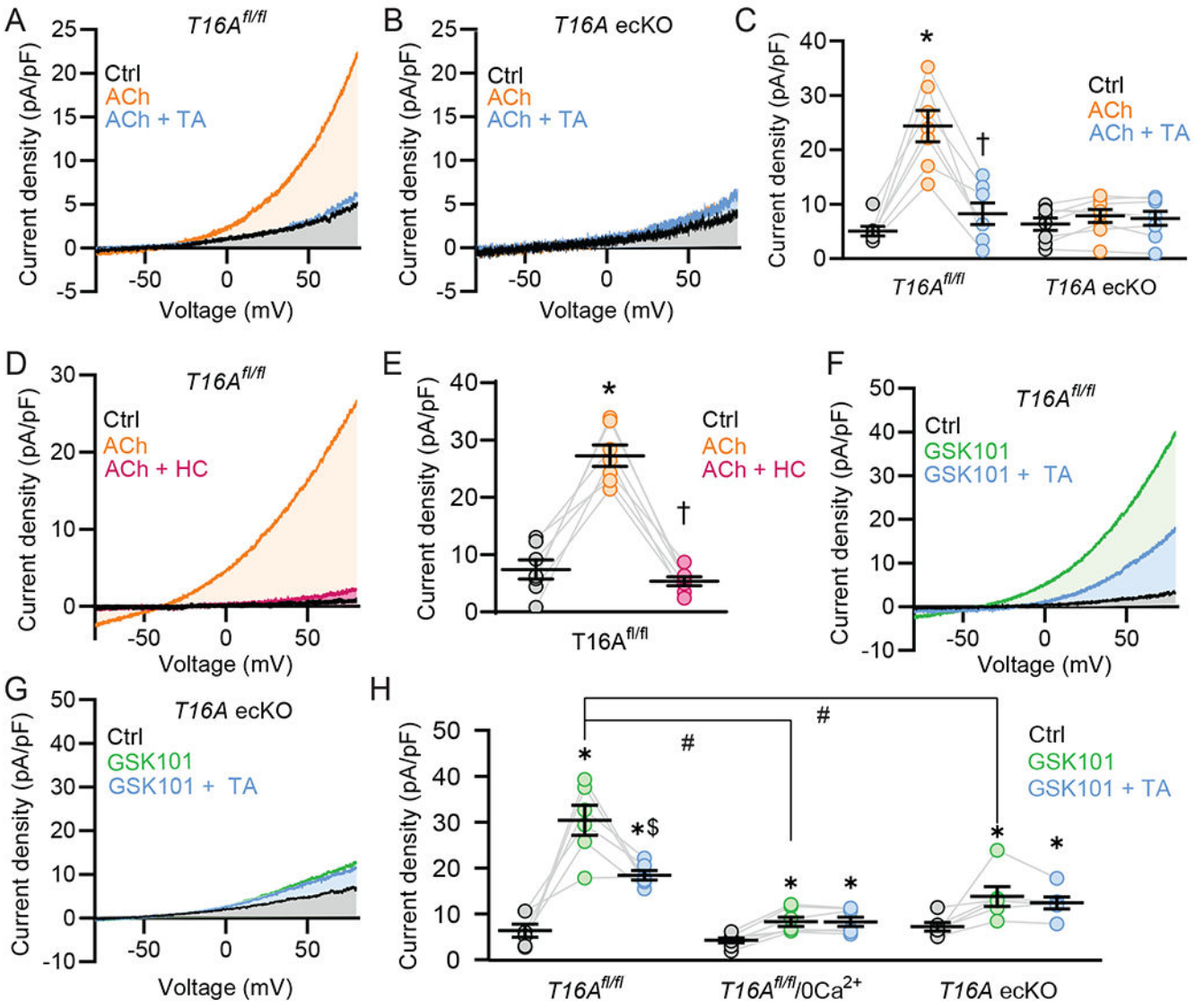

Fig. 2. ACh activates TRPV4-dependent TMEM16A currents in ECs.

(**A** and **B**) Representative whole-cell current recordings of freshly isolated endothelial cells from *TMEM16A*$^{fl/fl}$ (*T16A*$^{fl/fl}$, A) and *TMEM16A* ecKO (*T16A* ecKO, B) mice before and after applying ACh (10 μM) and ACh (10 μM) + tannic acid (TA, 10 μM). (**C**) Mean data at +80 mV from experiments in (A) and (B). N=7 cells from 6 *TMEM16A*$^{fl/fl}$ mice and n=6 cells from 6 *TMEM16A* ecKO mice. *, p<0.05 compared to pretreatment; †, p<0.05 compared to ACh. (**D**) Representative whole-cell current recordings of a freshly isolated endothelial cell from a *TMEM16A*$^{fl/fl}$ mouse before and after the addition of ACh (10 μM) and ACh (10 μM)+HC067047 (HC, 1 μM). (**E**) Mean data at +80 mV from experiments in (D) (n=7 cells from 6 *TMEM16A*$^{fl/f}$ mice). *, p<0.05 compared to pretreatment; †, p<0.05 compared to ACh. (**F** and **G**) Representative whole-cell current recordings in freshly isolated endothelial cells from *TMEM16A*$^{fl/fl}$ (F) and *TMEM16A* ecKO (G) mice before and after the addition of GSK101 (1 nM) or GSK101 (1 nM) + TA (10 μM). (**H**) Mean data at +80 mV from experiments in (F) (n=6 cells from 6 *TMEM16A*$^{fl/fl}$ mice) and (G) (n= 6 cells

from 5 *TMEM16A* ecKO mice). Mean data at +80 mV from whole-cell current recordings in freshly isolated endothelial cells from *TMEM16A*$^{fl/fl}$ mice before and after applying GSK101 (1 nM), and GSK101 (1 nM) + TA (10 μM) with $[Ca^{2+}]_o$ = 0 (n=7 cells from 4 mice). *, P<0.05 compared to pretreatment; $, p<0.05 compared to GSK101; #, p<0.05.

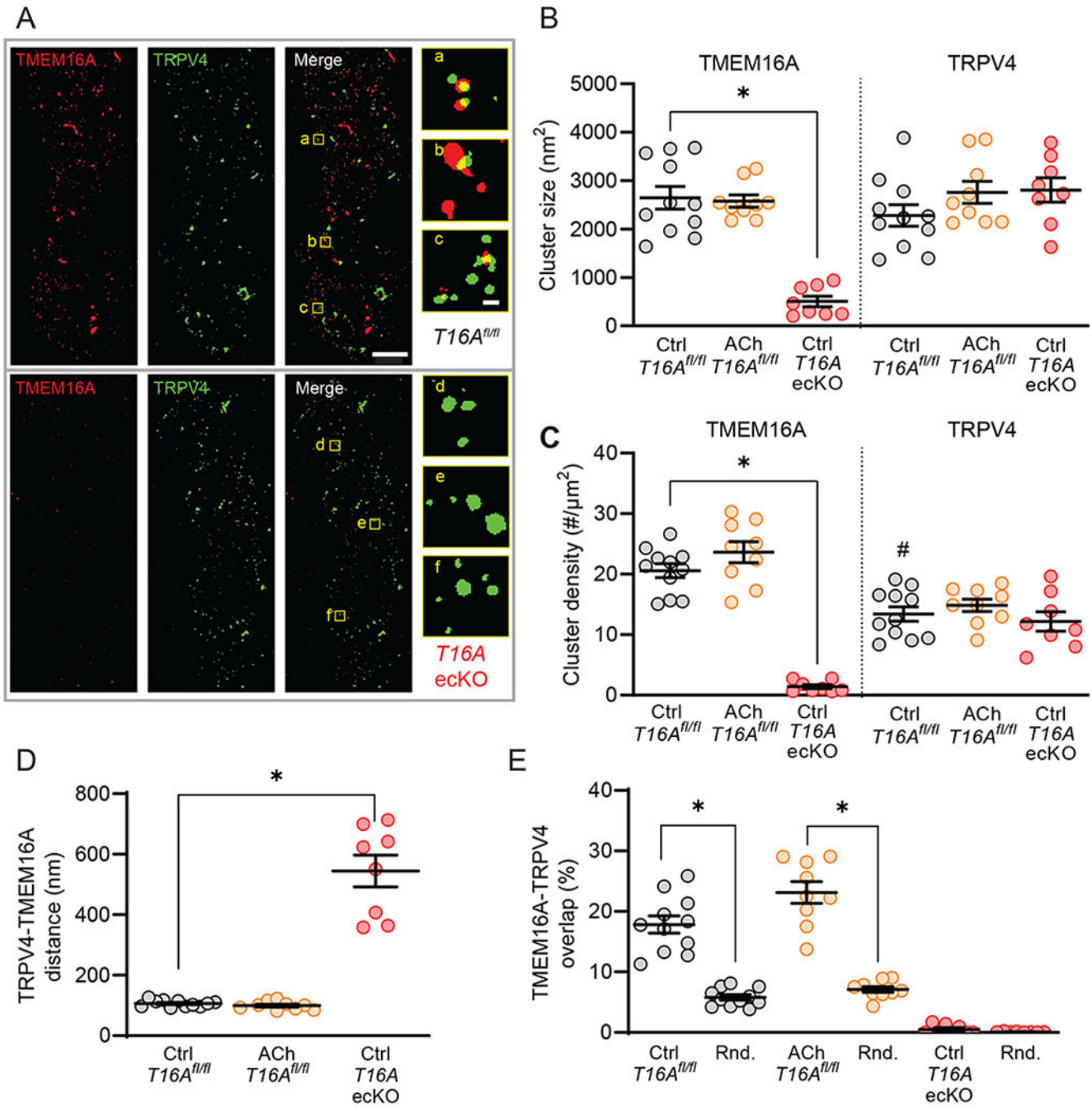

Fig. 3. Plasma membrane TMEM16A and TRPV4 clusters locate in nanoscale proximity in endothelial cells.

(**A**) TIRF-SMLM images of TMEM16A and TRPV4 surface clusters in freshly isolated mesenteric artery endothelial cells from *TMEM16A*$^{fl/fl}$ (*T16A*$^{fl/fl}$) and *TMEM16A* ecKO (*T16A* ecKO) mice. Scale bars are 2 μm for the whole cell images and 100 nm for the inset images on the right. (**B**) Mean data for TMEM16A and TRPV4 cluster sizes. *, P<0.05. (**C**) Mean data for TMEM16A and TRPV4 cluster density. *, P<0.05, #, P<0.05 compared to Ctrl *TMEM16A*$^{fl/fl}$. (**D**) Mean data for TMEM16A to TRPV4 nearest-neighbor cluster

analysis. *, P<0.05. (**E**) Mean data for the percentage of TMEM16A clusters that overlap with a TRPV4 cluster. Also illustrated is TMEM16A to TRPV4 overlap following Coste's randomization (Rnd) simulation. The number of cells analyzed in each condition is: 11 *TMEM16A*$^{fl/fl}$ cells, 9 *TMEM16A*$^{fl/fl}$ cells exposed to 10 μM ACh and 8 *TMEM16A* ecKO cells from 6 *TMEM16A*$^{fl/fl}$ mice and 5 *TMEM16A* ecKO mice. *, P<0.05.

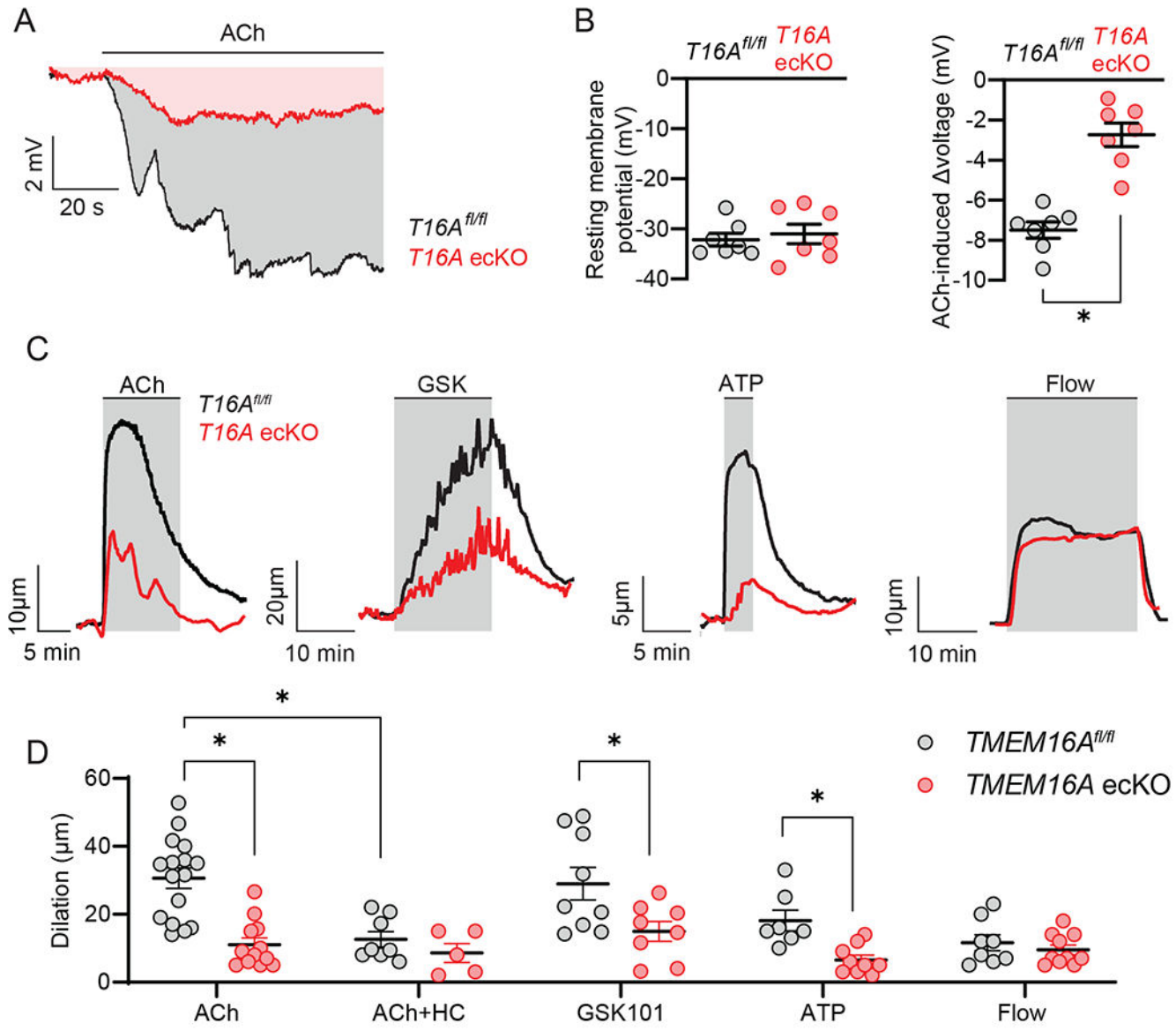

Fig. 4. TMEM16A channel activation in endothelial cells contributes to ACh-induced arterial hyperpolarization and vasodilation.

(**A**) Representative membrane potential recordings obtained from microelectrode impalements in pressurized (80 mmHg) mesenteric arteries from *TMEM16A*$^{fl/fl}$ (*T16A*$^{fl/fl}$) and *TMEM16A* ecKO (*T16A* ecKO) mice treated with ACh (10 μM). (**B**) Mean data obtained from experiments in (A) showing the membrane potential in control and the magnitude of the ACh-induced hyperpolarization in mesenteric arteries of *TMEM16A*$^{fl/fl}$ (n=7 mesenteric arteries from 6 mice) and *TMEM16A* ecKO mice (n=7 mesenteric arteries from 5 mice). *, P<0.05. (**C**) Representative traces illustrating diameter responses of pressurized (80 mmHg) mesenteric arteries from *TMEM16A*$^{fl/fl}$ and *TMEM16A* ecKO mice treated with ACh (10 μM), GSK101 (10 nM), ATP (1 μM) or intravascular flow (15 dyn/cm^2). (**D**) Mean data obtained from experiments in (C) showing dilation in response to ACh (n=16 mesenteric arteries from 14 *TMEM16A*$^{fl/fl}$ mice, n=12 mesenteric arteries from

11 *TMEM16A* ecKO mice), ACh + HC067047 (HC, 1 μM) (n=8 mesenteric arteries from 8 *TMEM16A*$^{fl/fl}$ mice, n=5 mesenteric arteries from 5 *TMEM16A* ecKO mice), GSK101 (n=9 mesenteric arteries from 9 *TMEM16A*$^{fl/fl}$ mice, n=8 mesenteric arteries from 7 *TMEM16A* ecKO mice), ATP (n=7 mesenteric arteries from 7 *TMEM16A*$^{fl/fl}$ mice, n=9 mesenteric arteries from 8 *TMEM16A* ecKO mice) and intravascular flow (n=8 mesenteric arteries from 7 *TMEM16A*$^{fl/fl}$ mice, n=10 mesenteric arteries from 9 for *TMEM16A* ecKO mice). *, $P<0.05$.

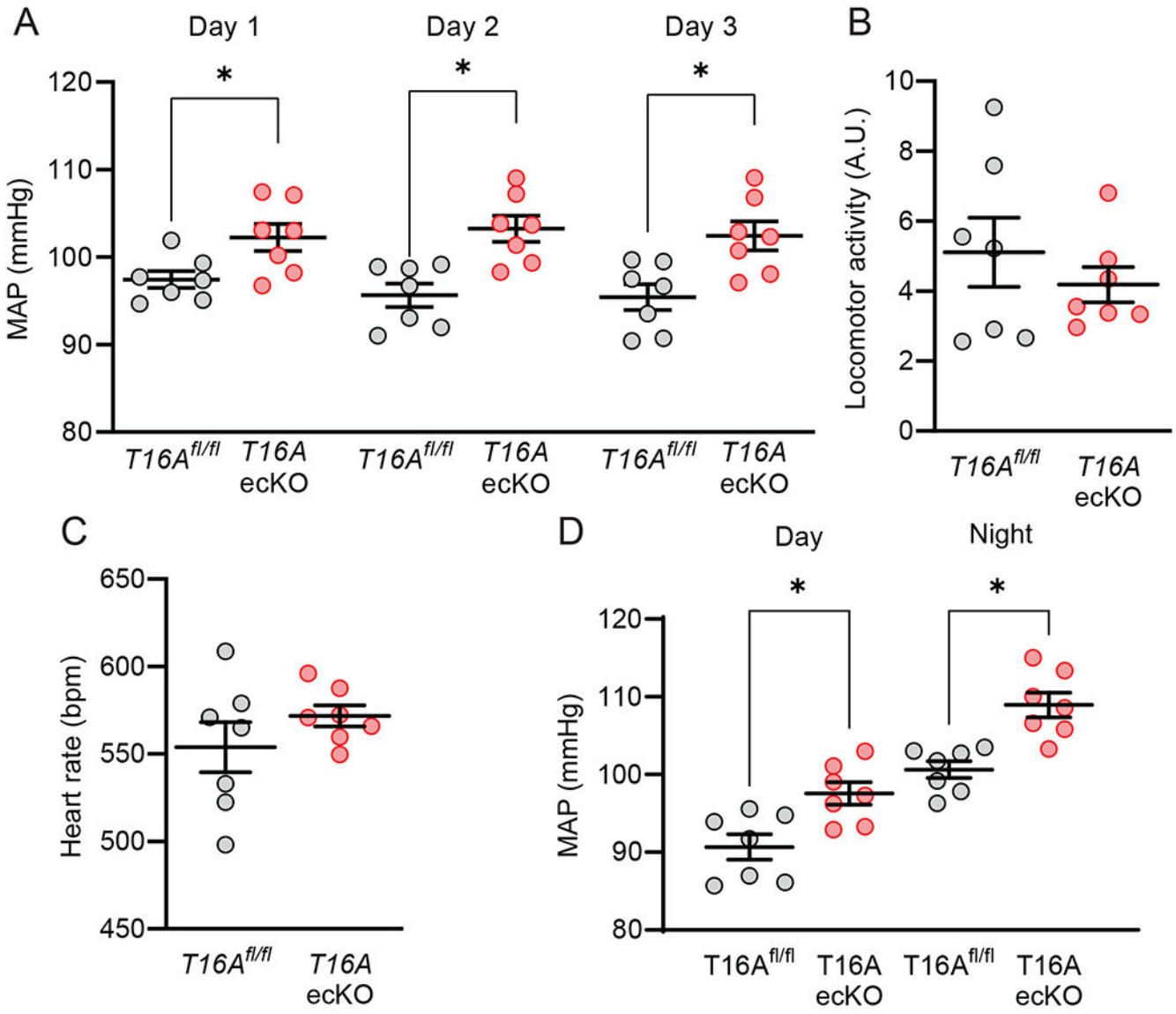

Fig. 5. Endothelial cell-specific TMEM16A knockout increases blood pressure.

(**A**) Mean arterial blood pressure (MAP) over a consecutive 3 day time period 14-16 days after the last tamoxifen injection in *TMEM16A*$^{fl/fl}$ (*T16A*$^{fl/fl}$) and *TMEM16A* ecKO (*T16A* ecKO) mice. N=7 mice per group. *, P<0.05. (**B**) Mean data of locomotor activity. N=7 mice per group. (**C**) Mean heart rate. N=7 mice per group. (**D**) MAP measured during day (inactive) and night (active) periods in *TMEM16A*$^{fl/fl}$ and *TMEM16A* ecKO mice 14 days after the last tamoxifen injection. N=7 mice per group. *, P<0.05.

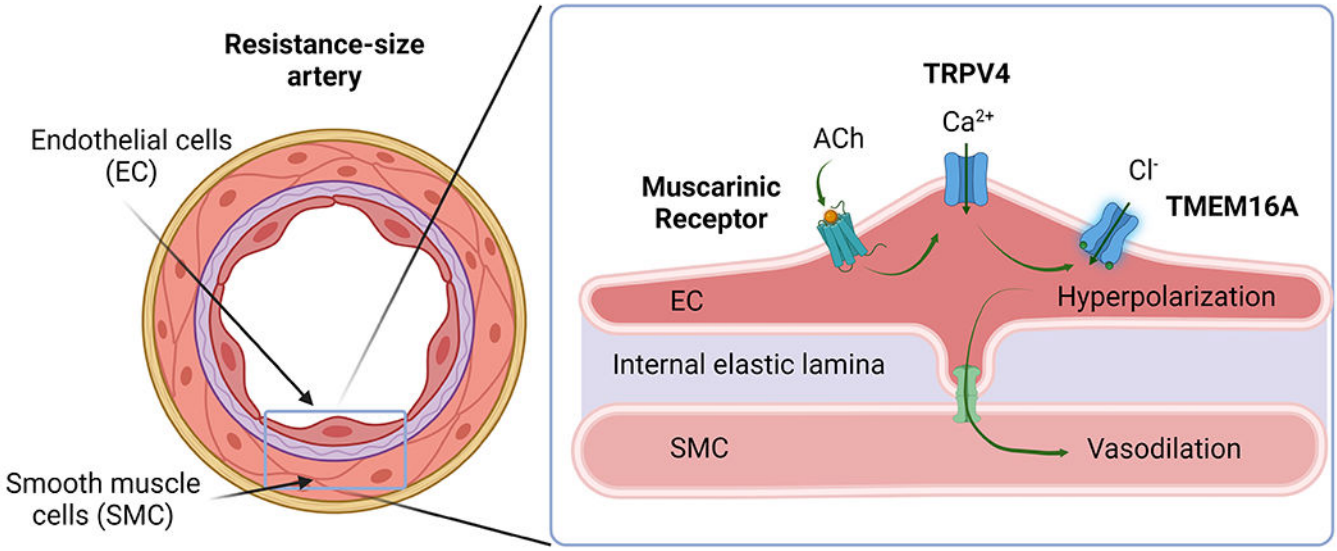

Fig. 6. TMEM16A channel activation in endothelial cells elicits vasodilation.

ACh activates TRPV4 channels, leading to Ca^{2+} influx which stimulates nearby TMEM16A channels in endothelial cells. The resulting membrane hyperpolarization relaxes arterial smooth muscle cells, leading to vasodilation and a reduction in blood pressure. ACh, acetylcholine; TRPV4, transient receptor potential vanilloid channel 4; TMEM16A, transmembrane protein 16A; EC, endothelial cell; SMC, smooth muscle cell.